MALAYSIAN JOURNAL OF MICROSCOPY

Journal homepage: https://malaysianjournalofmicroscopy.org

RESEARCH ARTICLE

EFFECT OF CONTROLLED TEMPERATURE ON SURFACE PROPERTIES OF ANODIC ALUMINUM OXIDE COMPOSITE COATING

Hasnol Hadi Zakaria[1], Shahira Liza[1,*], Kanao Fukuda[1], Noor Ayuma Mat Tahir[1], Yazid Yaakob[2]

[1]Malaysia-Japan International Institute of Technology, Universiti Teknologi Malaysia, Jalan Sultan Yahya Petra, Kampung Datuk Keramat, 54100, Kuala Lumpur, Malaysia.

[2]Department of Physics, Faculty of Science, Universiti Putra Malaysia, 43400 UPM Serdang, Selangor, Malaysia.

Abstract. Bi-layered coating strategies for carbon-based materials reinforcement of composite oxide coatings show promise for producing long-lasting durable materials. The bi-layered coating comprises an oxide/graphite lubricant composite (top layer) and Diamond-like carbon (DLC)-contained oxide coating (sub-layer). Reinforcement particles contribute to the oxide coating by filling pores formed after anodizing; however, they do not alter the porous structure. However, the porous structure can be regulated by adjusting the electrolyte temperature, as anodizing temperature influences the growth and morphology of the oxide coating. A higher electrolyte temperature can increase porosity, which leads to hardness reduction. This study aims to control electrolyte temperature and examine the porous structure of the bi-layered composite oxide coating. The bi-layered composite oxide coating was fabricated on aluminum alloy (AA2017-T4) by anodizing method with various constant electrolyte temperature (30 ℃, 40 ℃, 50 ℃ & 60 ℃). The surface roughness of the oxide coating measured by 3D optical profiler where it affected by the pore dimension of the oxide layer. Then the microhardness was measured by using the Vickers hardness test. The pore dimension of the oxide layer showed reduction. The microhardness increased approximately up to twofold (from 205.8 HV to 413.4 HV) for conventional oxide coating and up to 25.10% (from 345.8 HV to 432.7 HV) for bi-layered composite oxide coating when compared between uncontrolled electrolyte temperature with controlled electrolyte temperature due to densification of the oxide film occur when the temperature of the electrolyte during the anodization controlled, especially at 50 ℃ where the highest microhardness achieved. Therefore, this finding will contribute to automotive applications as it enhanced the properties of the aluminum alloy where it is widely used in aircraft and automotive parts.

Keywords: Anodizing, composite coating, roughness.

Article Info

Received 27 February 2025
Accepted 9 May 2025
Published 2 June 2025

***Corresponding author: shahiraliza@utm.my**

ISSN: 1823-7010, eISSN: 2600-7444

1. INTRODUCTION

Aluminum alloys are favored in the automotive and aerospace industries due to their lightweight, high strength and corrosion resistance [1]. However, it still has limitations such as low surface hardness, ease of scratch, and low wear resistance. These limitations can be overcome by applying surface modification to the aluminum alloy.

One of the surface modifications that can be applied to enhance aluminum alloy surface properties is anodizing. Anodizing is an electrochemical process to form a protective anodic film on metal surface that enhanced the corrosion and wear resistance [2]. Anodizing can achieve higher hardness and strength while also providing good protective and decorative surface properties with a thicker oxide layer as high as 125 μm of thickness. However, the anodized oxide film also known as anodic aluminum oxide (AAO) still cannot achieve the best mechanical performance due to the porous structure of the film.

Al alloys are classified into a few series such as 2XXX, 6XXX and 7XXX group where the oxide coating formed on these Al alloys during anodizing are affected by intermetallic phases such as Al_2Cu, Al_2CuMg, Al_7Cu2Fe, $Al_4Cu_2Mg_8Si_7$, AlCuFeMnSi, and Mg_2Si [3]. The high copper and silicon content in Al alloys contribute to the porous structure of the AAO coating. According to Bononi et al. [4], the sites enriched with copper enhanced oxygen evolution activity in the oxide layer and have a significant impact on reducing the anodizing efficiency. The oxygen evolution activity occurs during anodizing process, causing porous structures to form. Other than that, AAO also faces another problem, which is fatigue cracks on the surface or at internal sites. Fatigue cracks may form due to the presence of various intermetallic phases, which affect the uniformity of oxide layer growth [5]. The intermetallic phase can hinder the uniformity of the oxide layer formation that leads to complex porosity and uneven oxide growth with cracked oxide layers [6].

Recently, there have been approaches to reduce the porosity by adding reinforcement particles into the AAO coating. Reinforcing carbon-based materials like graphite, graphene and diamond-like carbon into the AAO coating are proven can reduce the porosity and increase the microhardness [7-9]. The particles embedded in the oxide film led to densification of the coating. Studies have also fabricated composite coatings using pulse current (PC) anodization to mitigate fatigue cracks and porosity issues [10]. PC anodization has proven to reduce crack, and porosity leads to an increased in the mechanical strength of the coating by 25.20% compared to the direct current (DC) anodizing method [10]. The mechanical strength improvement is due to the recovery effect that occur when using the pulse current method that allow efficient dissipation of heat generated on the surface of the anodized aluminum [11]. The same method has also been done by Zulkifli et al. [9] except that they used diamond-like carbon as reinforcement particles. As a result, denser and more uniform film was produced.

Even though adding reinforcement particles into the AAO coating can reduce the porosity up to 43.20% for width and 58.80% for depth, and improve the coating microhardness [10], the microhardness values are still considered as low because, according to Sathiyakumar [12], theoretically, the microhardness of alumina ceramic is about 1020 HV. The difference occurs due to residual pores that still exist within the AAO coating even after the dimension of the pores reduced with the aid of the reinforcement particles. The result achieved shows that still less than half of the pores dimension managed to be reduced by the reinforcing particles.

One of the concerns on why the pore dimension still cannot be reduced more than half even after applying pulse current method and adding reinforcement particles may be due to electrolyte temperature. As stated by Dobosz [13], the rate of pore widening depends on the type of electrolyte and anodizing condition especially anodizing voltage and temperature used. Increasing electrolyte temperature accelerates oxide growth; however, it also enhances aluminum oxide dissolution, leading to a more porous structure. The increased of oxide dissolution due to increasing electrolyte temperature leads to a more porous oxide structure.

This issue emphasizes the requirement for further improvement of the anodizing process especially to minimize the porosity of the AAO coating to improve its mechanical properties. Recently, fabricating bi-layered coating has been done and proven to improve the mechanical properties by using two different reinforcement particles. Our approach is to combine graphite/oxide layer as top layer, and DLC/oxide as sub layer. This approach is considered based on the findings from our previous work [8-10,14]. In this study, the aim is to improve the mechanical properties of the AAO coating by fabricating bi-layered coating and controlling electrolyte temperature, as well as examine the porous structure of the coating.

2. MATERIALS AND METHODS

2.1 Materials and Preparation

The substrate used for the anodizing process was the AA2017-T4 Al alloy discs purchased from Misumi Malaysia Sdn. Bhd, which has a 25 mm diameter and a 4 mm thickness. The primary alloying element in AA2017-T4 aluminum alloy is copper (Cu), with a chemical composition of 5.19% Cu, 91.79% Al, and 3.02% O. Prior to anodizing, the substrates were mechanically polished using silicon carbide (SiC) abrasive papers, progressing from 600 to 2000 grit. They were then ultrasonically cleaned in distilled water, ethanol, and acetone for 10 minutes each, with the process repeated twice. In this study, DLC-deposited Cu particle and graphite flakes used as reinforcement particles. The SEM images of graphite flakes and DLC-deposited Cu particle are shown in Figure 1. The DLC-deposited CU particle was fabricated by chemical vapor deposition (CVD). Copper particles were placed in a vacuum chamber on a stainless-steel tray that acted as a negative electrode. Acetylene gas used as gas precursor with applied voltage maintained at -3.5 kV. The deposition time of DLC on copper particles was set at 30 min. The copper particles were agitated three times every 10 min during the deposition process. The copper from the DLC-deposited Cu particle then dissolved in electrolyte during anodizing as the copper only act as carrier.

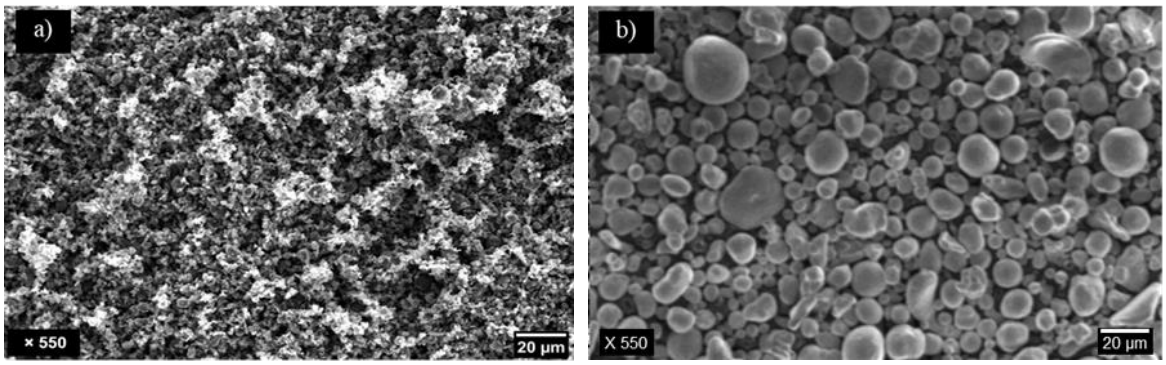

Figure 1: Surface morphology of (a) graphite particles (400 nm – 600 nm) and (b) DLC-deposited Cu particle

2.2 Experimental Set-up

The study utilized a PC power supply with a unidirectional square wave pulse for the anodizing process. The electrolyte used was a solution of sulfuric acid (H_2SO_4) that had been diluted with distilled water to a concentration of 20 wt%. 1 g/L of DLC-deposited Cu particles were mixed into electrolyte to fabricate the first layer of the composite coating. While for the second layer of composite coating where graphite flakes used as reinforcement, 20 mL/L of ethanol used to disperse the graphite flakes and stirred with magnetic stirrer for 20 min at 200 rpm.

AA2017-T4 Al alloy substrate was used as the anode while SUS 316 L stainless steel plate used as the cathode to complete the circuit. Before anodizing, the temperature of the electrolyte was set constant at 30 ℃, 40 ℃, 50 ℃ and 60 ℃. The anodizing process was carried out for 60 min for

conventional oxide coating while for composite bi-layer coating are 30 minutes for the first layer and another 30 minutes for the second layer. By using PC power supply, the interval time on is 30 seconds and the time off is 10 seconds with 15 A/dm^2 of constant current density and 15 V initial voltage.

2.3 Surface Characterization

3D optical profiler ZeGage^{TM} (Zygo Corporation and Ultra Precision Technology Division of AMETEK Inc., United States) was used to analyze the surface topography images to determine the surface roughness and pore dimensions. The scanning electron microscopy (SEM) JSM-6010PLUS/LA (JEOL Ltd, Japan) was utilized to observe the surface morphology of the coating. Then the mechanical properties of the coating was measured by Vickers hardness machine (Shimadzu Corporation, Japan) with applied load of 0.1 HV for a duration of 10 seconds. The Vickers indenter is a regular quadrangular pyramid diamond with an angle between opposing faces of 136 degrees. To ensure the accuracy of the microhardness value, approximately 15 points of microhardness indention have been done.

3. RESULTS AND DISCUSSION

3.1 Surface Characterization

Figure 2 represents the SEM images and 3D profiles of conventional oxide coating surfaces anodized at different controlled temperatures, which are 30 ℃, 40 ℃, 50 ℃, 60 ℃ & uncontrolled temperature by pulse current for 60 minutes. The crests and troughs of a topographic picture are represented by a sequence of colour areas arranged in the following order: red, orange, yellow, green, and blue [14]. The red region indicates the area's greatest height (crest), while the blue region denotes the lowest area (trough). The average Ra value of oxide coatings anodized at 30 ℃, 40 ℃, 50 ℃, 60 ℃ and uncontrolled temperature was 2.57, 4.42, 4.74, 14.21 and 10.43 μm, respectively, as illustrated in Figure 3.

Based on Figure 2, oxide coating that anodized at 30 ℃ dominated by pits compared to other samples that dominated by pores. As the anodizing temperature increased to 40 ℃, undulation started to occur on the coating surface as can be seen in the Figure 2(b). In Figure 2(c), the undular structure on the coating surface become more obvious where the anodizing temperature was set constant at 50 ℃. Undular structure is wave-like morphology on the surface. At 60 ℃, the coating surface exhibits a different morphological structure compared to undular structures that resulted from lower electrolyte temperatures. The surface structure transitioned to different appearances, most likely due to changes in growth and oxide dissolution rate. On the other hand, oxide coating that anodized with uncontrolled (UC) temperature shows a similar surface structure with oxide coating anodized at 60 ℃. This might be happened due to its temperature that can increase up to 61.1 ℃ even though the initial temperature was set at room temperature.

Based on Figure 3, the highest surface roughness was obtained from oxide coating anodized at 60 ℃ while the lowest surface roughness was obtained from oxide coating anodized at 30 ℃. The trend of the surface roughness corresponding to the size of the pores where the largest pore dimensions were obtained from oxide coating anodized at 60 ℃ while the smallest pore was obtained from oxide coating anodized at 30 ℃ as (Figure 4). The width and depth of pores obtained on oxide coating anodized at 60 ℃ is 116.37 and 102.93 μm, respectively. For controlled electrolyte temperatures anodizing, the pore dimension increased linearly with electrolyte temperatures. This is because the rate of pore widening depends on the type of electrolyte and anodizing condition, especially anodizing voltage and temperature used. The increasing electrolyte temperature increases oxide dissolution that leads to a more porous structure. In relation to the increment of pore dimensions, larger pores lead to higher surface roughness. The huge pore dimension of oxide coating anodized at 60 ℃ explained why the surface roughness of the oxide coating shown a significant difference compared to other oxide coating.

Furthermore, the formation of craters on the oxide coating resulted from a combination of large pores [15] and undulation structure also lead to higher surface roughness.

Generally, the porous structure developed after formation of non-porous barrier layer. During the formation of the porous oxide layer, oxide formation and dissolution occur simultaneously [16]. According to Scheer et al. [17], the dissolution of the oxide layer occur at the interface between the oxide layer and the electrolyte due to weakening of Al-O bonding in the oxide lattice. On the other hand, pits that can be seen on the coating surface that anodized at 30 ℃ may cause by dissolution of intermetallic phase during the anodizing process.

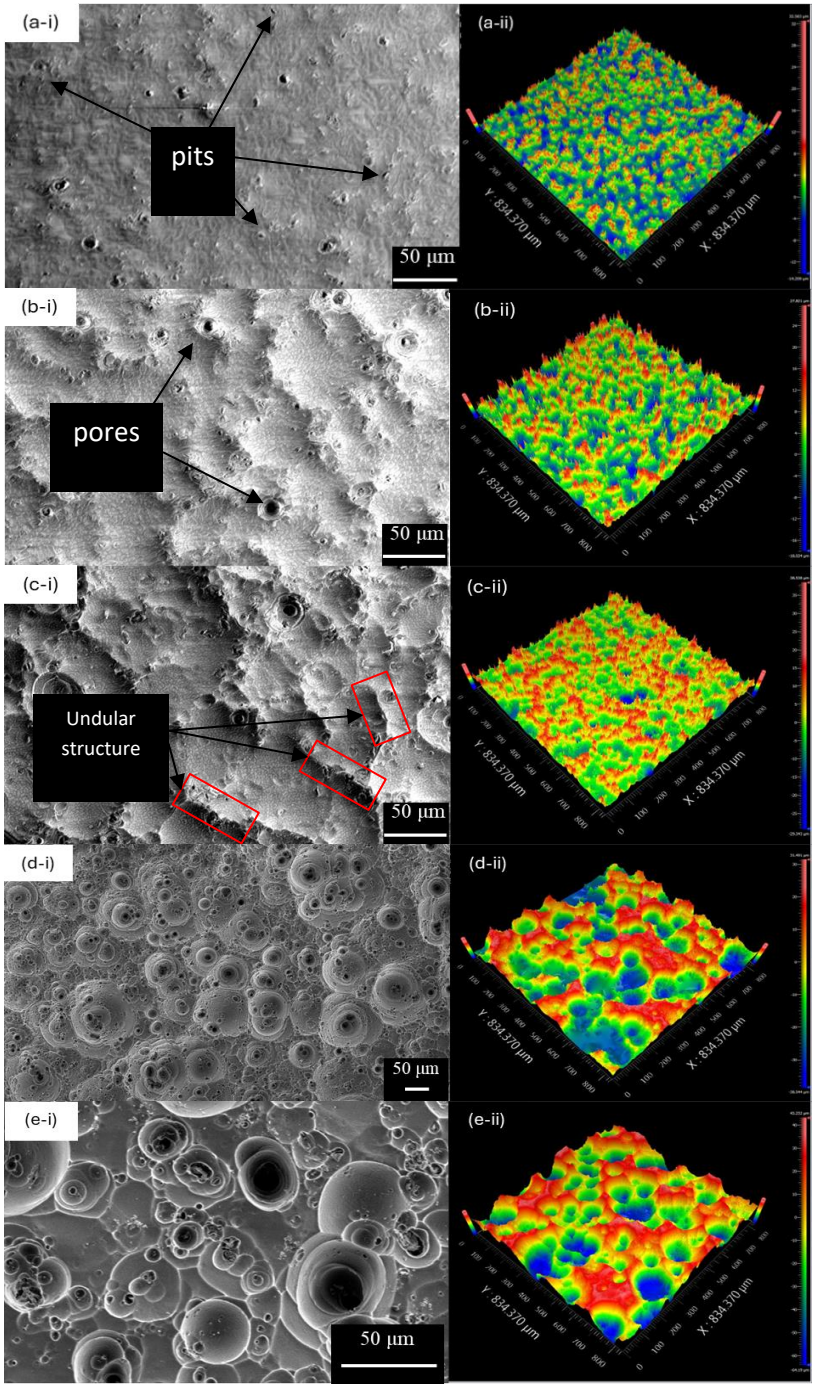

Figure 2: SEM images and 3D profiles of conventional oxide coating surface with (a) 30 ℃, (b) 40 ℃, (c) 50 ℃, (d) 60 controlled temperature and (e) uncontrolled temperature

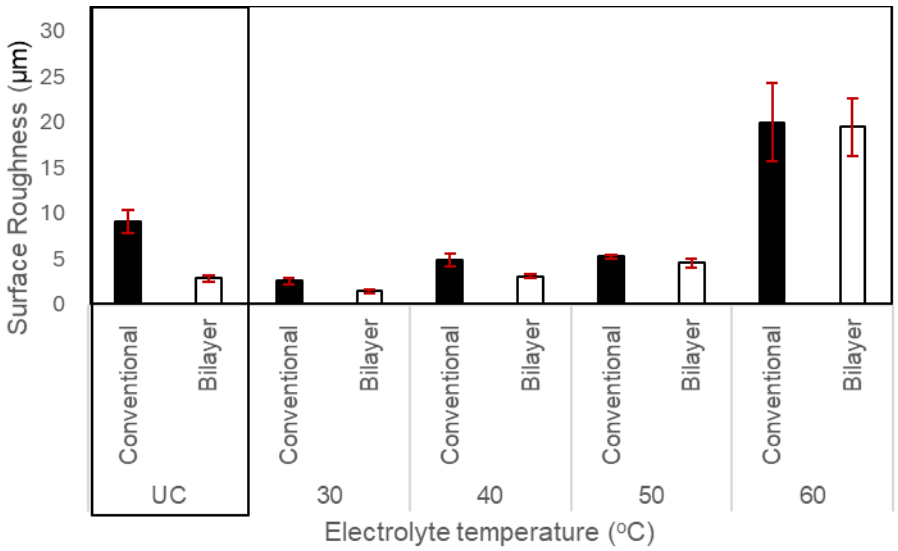

Figure 3: Average surface roughness of uncontrolled temperature composite bilayer coating and conventional oxide coating, controlled temperature conventional oxide coating and composite bilayer coating

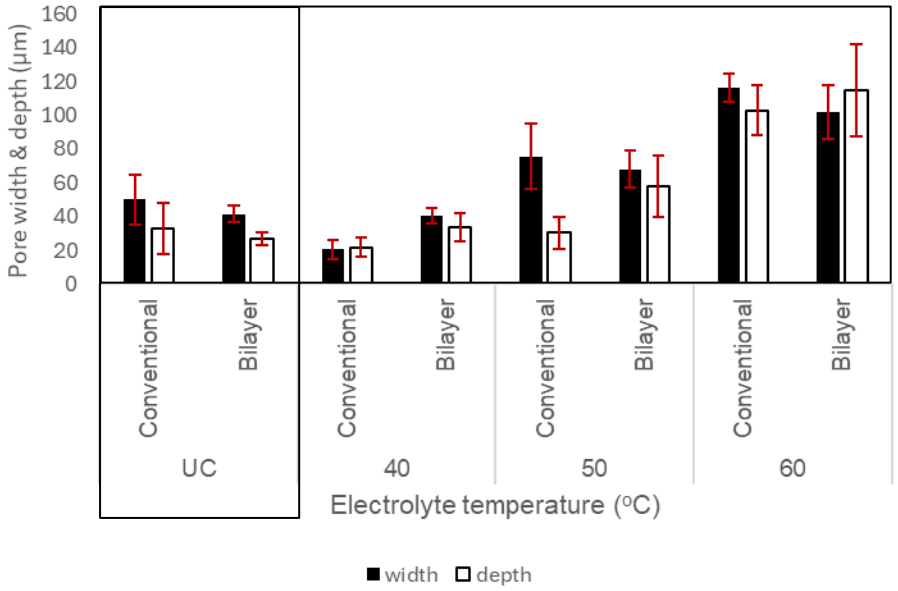

Figure 4: Average pore dimension of controlled temperature conventional oxide coating and composite bilayer coating

On the other hand, Figure 5 represents the SEM images and 3D profiles of composite bilayer coating surfaces anodized at different controlled temperatures which is 30 ℃, 40 ℃, 50 ℃, 60 ℃ & uncontrolled temperature by pulse current for 30+30 minutes. The SEM images of the composite bilayer coating show similar trend with the conventional oxide coating where the surface dominated by pits at 30 ℃ as shown in Figure 2(a) and Figure 5(a). Then at 40 ℃, the coating surface started to dominate by pores as shown in Figure 2(b) and Figure 5(b). Despite the pore formation, undulation also started to occur for composite bilayer coating at 40 ℃ as can be seen in Figure 5(b). As the anodizing temperature increased to 50 ℃, the undular structure is more apparent.

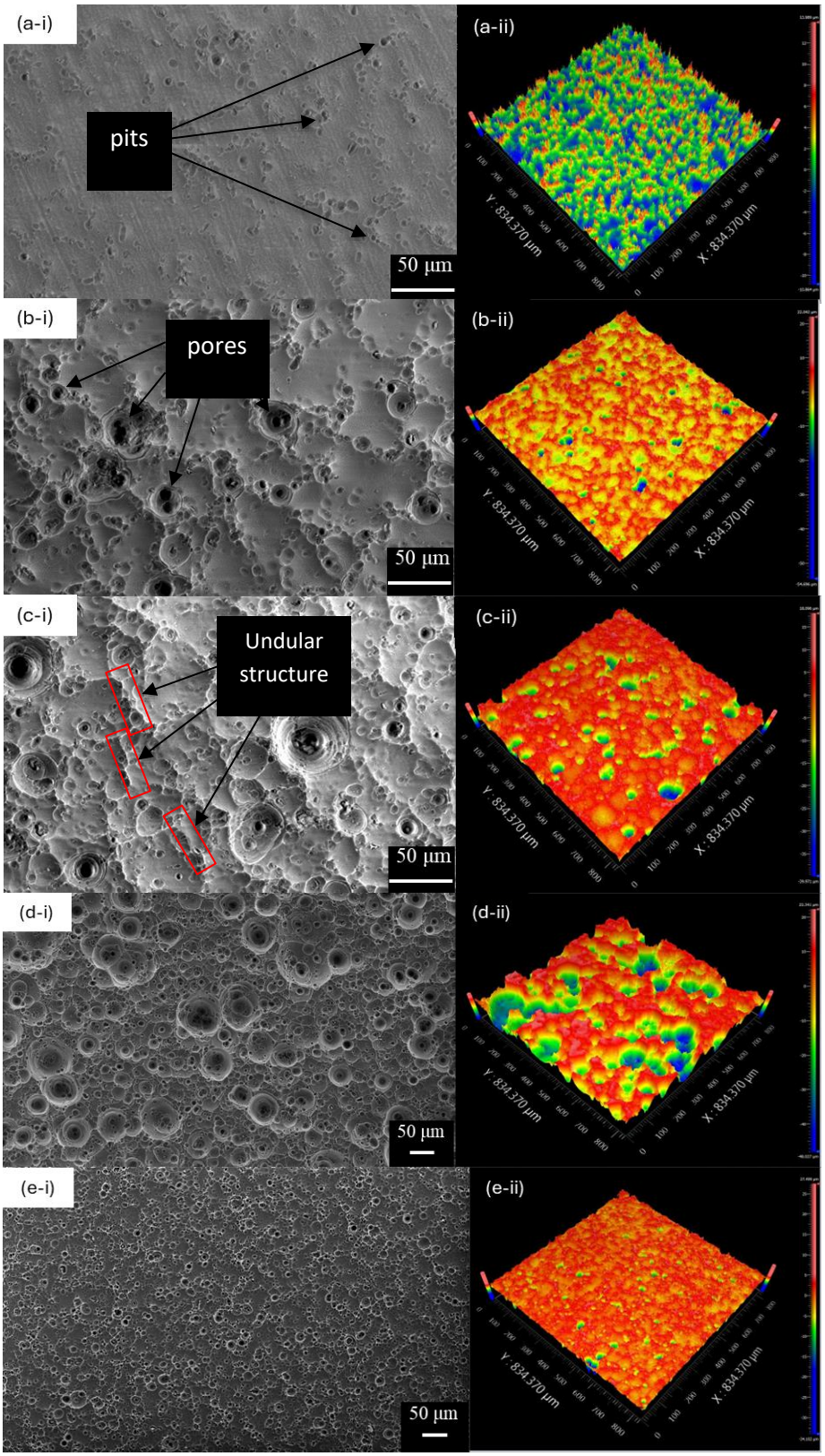

Figure 5: SEM images and 3D profiles of composite bilayer coating surface with (a) 30 ℃, (b) 40 ℃, (c) 50 ℃, (d) 60 ℃ controlled temperature and (e) uncontrolled temperature

Other than that, unlike the conventional oxide coating, the composite bilayer coating shows different surface topography trend. At 40 ℃, the composite bilayer coating dominated by red zone and no spikes seen on the 3D profiles image as shown in Figure 5(b). Meanwhile, Figure 2(b) shows that

the conventional oxide coating dominated by green region and many spikes. The different topography caused by higher electrolyte conductivity during the anodization of the composite bilayer coating. According to Mohamad et al. [14], the dispersion of graphite in the electrolyte lead to increasing of electrolyte conductivity due to good electrical conductivity of the graphite. The higher electrolyte conductivity of the composite bilayer coating causes the oxide dissolution to increase. The spike that can be seen at 30 ℃ in the 3D profiles image for the composite bilayer coating which is the protrusion seems to be flattened at 40 ℃ due to oxide dissolution occur at the protrusion. The average Ra value of composite bilayer coatings anodized at 30 ℃, 40 ℃, 50 ℃, 60 ℃ and uncontrolled temperature was 1.46, 2.96, 4.84, 13.38 and 2.92 µm, respectively, as illustrated in Figure 5. Most of the composite bilayer coating shows slight reduction in the surface roughness value due to the presence of reinforcement particles both inside and surrounding the pores, which caused a notable decrease in surface roughness [15].

The incorporation of the reinforcement particles caused the pore dimension of the composite bilayer coating slightly reduced compared to conventional oxide coating as shown in Figure 6. The largest pore dimension obtained for composite bilayer coating when anodized at 60 ℃ with 101.84 µm in width and 114.81 µm in depth compared to 116.37 µm in width and 102.93 µm in depth for conventional oxide coating that also anodized at 60 ℃. The reduction in pore dimensions occur due to incorporation of DLC and graphite particles into the pore. This finding also supported by Mohamad et al. [14] that reported a significant reduction in pore dimensions and surface roughness on the composite Al_2O_3 coatings after increasing the graphite content. Rawian et al. [8] also found that the reduction in the formation of pores associated with incorporating DLC deposited on Cu particles inside and around the pores, which resulted in a considerable decrease in surface roughness. The incorporation of the particles in the oxide coating can be done by mechanical entrapment mechanism where the particles entrapped during the oxide coating formation and entrapped within the pores. Similar mechanism was introduced by Chen et al. by using Al_2O_3 and PTFE particles inside oxide coating [18]. Figure 6 shows the graphite particles entrapped into the pores. The graphite presence in the pores are confirmed by EDS analysis as shown in Table 1.

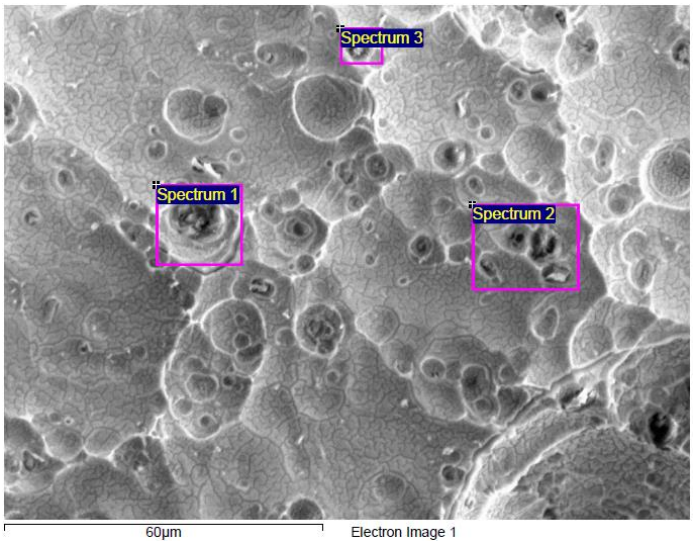

Figure 6: SEM images of graphite particles embedded into composite bilayer coating surface

Table 1: Chemical compositions of the composite bilayer coating

	Weight %		
Spectrum	**C**	**O**	**Al**
1	3.75	58.45	37.8
2	3.18	54.7	42.12
3	2.81	55.48	41.71

Based on Figure 4, it can be seen that the pore dimension increased as the anodizing temperature increased for both conventional and composite bilayer oxide coating. However, most of composite bilayer oxide coating produce smaller pores compared to conventional oxide coating that anodized at the same temperature. This finding indicates the reinforcement particle does help in reducing the pore size but smaller pore can be achieved at lower anodizing temperature. Even though temperature might be more dominant factor in reducing the pore size at lower anodizing temperature, the best mechanical properties cannot be achieved at lower anodizing temperature as shown in Figure 7. Judging from Figure 3 and Figure 4, increasing linear trend only can be seen as the temperature controlled increased up to 50 ℃, then discontinuity occur at 60 ℃ due to huge difference in surface roughness values.

3.2 Mechanical Properties

Microhardness of both composite bilayer coating and conventional oxide coating was measured by performing Vickers microhardness test on the surface of the samples. The comparison of the microhardness of each sample is shown in Figure 7. The highest microhardness value, 432.7 HV, was achieved by composite bilayer coating anodized at 50 ℃, followed by 413.4 HV microhardness value achieved by conventional oxide coating also anodized at 50 ℃. Anodizing at 30 ℃ until 50 ℃ shows an increasing trend in microhardness. However, at 60 ℃, the microhardness value suddenly decreased. The reduction in microhardness of the coating corresponds to its pore dimension (Figure 6), pore dimension produced at 60 ℃ anodizing was the largest compared to the others. This is important as the pore dimension of the coating affected its density, where the density of the materials is one of the factors that affect the microhardness of the oxide layer [19].

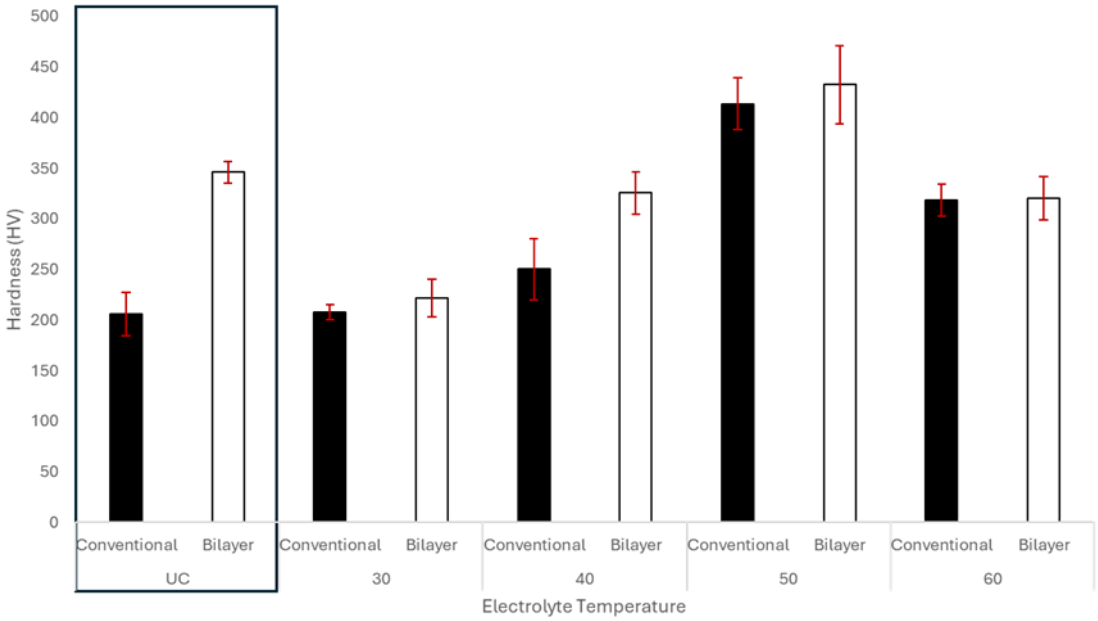

Figure 7: Average microhardness of uncontrolled temperature composite bilayer coating and conventional oxide coating, controlled temperature conventional oxide coating and composite bilayer coating

Furthermore, based on Figure 7, it can be seen that microhardness values of composite bilayer coating are higher than conventional oxide coating. One of the reasons for this is the density of the composite bilayer oxide coating higher than conventional oxide coating since its pore dimensions are smaller. Another reason is because of the reinforcement particles of the composite coating. The existence of the reinforcement particles in the coating structure improves the mechanical property of the coating [20]. The highest microhardness value achieved at 50 ℃ attributed to optimal microstructure achieved at this temperature with high density along with effective incorporation of reinforcement particles in the composite bilayer coating that contribute to enhanced mechanical properties.

4. CONCLUSIONS

In this study, conventional oxide coating and composite bilayer coating were fabricated by controlling the electrolyte temperature to improve the mechanical properties. Electrolyte temperature controlled at 50 ℃ is the optimal temperature of both conventional oxide coating and composite bilayer coating. The surface roughness of both conventional oxide coating and composite bilayer coating can be reduced up to 71.62% and 50.82%, respectively, when anodizing with controlled temperature compared to uncontrolled temperature. However, the surface roughness increased more than twofold for conventional oxide coating and more than fivefold for composite bilayer coating when the temperature controlled at 60 ℃. At 50 ℃, composite bilayer coating shows slight reduction in surface roughness values compared to conventional oxide coating. Up to 13.57% of reduction achieved by composite bilayer coating. The microhardness of conventional oxide coating increased up to twofold when anodizing with controlled temperature compared to uncontrolled temperature. On the other hand, the microhardness of composite bilayer coating shows improvement up to 25.10% when the temperature of the electrolyte controlled compared to the uncontrolled temperature. At 50 ℃, composite bilayer coating shows higher microhardness value compared with conventional oxide coating. Improvement of 4.67% was achieved by composite bilayer coating.

Acknowledgement

This research is supported by the grant from the Ministry of Higher Education, Malaysia under Fundamental Research Grant Scheme (FRGS/1/2023/TK10/UTM/02/11).

Author Contributions

All authors contributed toward data analysis, drafting and critically revising the paper and agree to be accountable for all aspects of the work

Disclosure of Conflict of Interest

The authors have no disclosures to declare

Compliance with Ethical Standards

The work is compliant with ethical standards

References

[1] Chen, J. (2023). Research on aluminum alloy materials and application technology for automotive lightweighting. *Academic Journal of Materials & Chemistry*, 4(6), 1-7.

[2] Malek, B., Chausummier, M. & Mabru, C. (2023). Effect of anodization and loading on fatigue life of 2618-T851 aluminum alloy. *International Journal of Fracture*. 240(2), 209-220.

[3] Zalnezhad, E., Sarhan, A. A. D. & Hamdi, M. (2013). Investigating the effects of hard anodizing parameters on surface hardness of hard anodized aerospace AL7075-T6 alloy using fuzzy logic approach for fretting fatigue application. *The International Journal of Advanced Manufacturing Technology*, 68(1-4), 453-464.

[4] Bononi, M., Conte, M., Giovanardi, R. & Bozza, A. (2017). Hard anodizing of AA2099-T8 aluminum-lithium-copper alloy: Influence of electric cycle, electrolytic bath composition and temperature. *Surface and Coatings Technology*, 325, 627-635.

[5] Shahzad, M., Chaussumier, M., Chieragatti, R., Mabru, C. & Rezai-Aria, F. (2011). Surface characterization and influence of anodizing process on fatigue life of Al 7050 alloy. *Materials & Design*, 32(6), 3328-3335.

[6] Bononi, M., Giovanardi, R., Bozza, A. & Mattioli, P. (2016). Pulsed current effect on hard anodizing process of 2024-T3 aluminium alloy. *Surface and Coatings Technology*, 289, 110-117.

[7] Yin, B., Peng, Z., Liang, J., Jin, K., Zhu, S., Yang, J. & Qiao, Z. (2016). Tribological behavior and mechanism of self-lubricating wear-resistant composite coatings fabricated by one-step plasma electrolytic oxidation. *Tribology International*, 97, 97-107.

[8] Rawian, N. A. M., Akasaka, H., Liza, S., Fukuda, K., Zulkifli, N. A., Tahir, N. A. M. & Yaakob, Y. (2023). Surface and tribological characterization of anodic aluminum oxide coating containing diamond-like carbon flakes. *Diamond and Related Materials*, 132*,* 109674.

[9] Zulkifli, N. A., Liza, S., Akasaka, H., Fukuda, K., Mohd Rawian, N. A., Md Ghazazi, N. A., Mat Tahir, N. A. & Yaakob, Y. (2023). Surface and tribology characterization of diamond-like carbon flakes reinforced oxide film by pulse anodizing. *Ceramics International*, 49(21), 34205-34222.

[10] Md. Ghazazi, N. A., Liza, S., Ishimatsu, J., Mat Tahir, N. A., Zulkifli, N. A. & Yaakob, Y. (2023). Effect of pulse current on surface properties of aluminum oxide coating containing graphite. *Surface and Interface Analysis*, 55(11), 831-844.

[11] Mustapar, N., Liza, S., Fukuda, K., Mat Tahir, N. A., Ishimatsu, J., Yaakob, Y. & Othman, I. S. (2024). Enhanced mechanical properties and tribological performance of anodic oxide coating by using thermal power plant waste material. *Ceramics International*, 50(20), 38372-38390.

[12] Sathiyakumar, M. & Gnanam, F. D. (2003). Influence of additives on density, microstructure and mechanical properties of alumina. *Journal of Materials Processing Technology*, 133(3), 282-286.

[13] Dobosz, I. (2021). Influence of the anodization conditions and chemical treatment on the formation of alumina membranes with defined pore diameters. *Journal of Porous Materials*, 28(4), 1011-1022.

[14] Mohamad, S., Liza, S. & Yaakob, Y. (2020). Strengthening of the mechanical and tribological properties of composite oxide film formed on aluminum alloy with the addition of graphite. *Surface and Coatings Technology*, 403, 126435.

[15] Mat-Tahir, N. A., Liza, S., Fukuda, K., Mohamad, S., Hashimi, M. Z. F., Mohd-Yunus, M. S., Yaakob, Y. & Othman, I. S. (2022). Surface and tribological properties of oxide films on aluminium alloy through fly-ash reinforcement. *Coatings*, 12(2), 256.

[16] Wankhede, S. & Pillai, D. S. (2024). Electrokinetics-driven anodic oxide pore formation: linear and weakly nonlinear analysis. *Journal of Electrochemical Society*, 171(11), 112501.

[17] Scheer, K. M., Tulloch, M., Hamam, I., Abraham, J. J., Johnson, M. B. & Metzger, M. (2025). Anodic dissolution of aluminum current collector in lithium-ion cells with LiFSI, LiPF6, and LiBF4. *Journal of The Electrochemical Society*, 172(1), 010511.

[18] Chen, S., Kang, C., Wang, J., Liu, C. & Sun, K. (2010). Synthesis of anodizing composite films containing superfine Al_2O_3 and PTFE particles on Al alloys. *Applied Surface Science,* 256(22), 6518-6525.

[19] Mohammadi, I., Afshar, A. & Ahmadi, S. (2016). Al_2O_3/Si_3N_4 nanocomposite coating on aluminum alloy by the anodizing route: Fabrication, characterization, mechanical properties and electrochemical behavior. *Ceramics International*, 42(10), 12105-12114.

[20] Wu, L., Wen, C., Zhang, G., Liu, J. & Ma, K. (2017). Influence of anodizing time on morphology, structure and tribological properties of composite anodic films on titanium alloy. *Vacuum*, 256, 176-184.